

Magnetic, Durable, and Superhydrophobic Polyurethane@Fe₃O₄@SiO₂@Fluoropolymer Sponges for Selective Oil Absorption and Oil/Water Separation

Lei Wu,^{†,‡,§} Lingxiao Li,^{†,‡} Bucheng Li,^{†,‡} Junping Zhang,^{*,†,‡} and Aiqin Wang^{*,‡}

[†]State Key Laboratory for Oxo Synthesis & Selective Oxidation, Lanzhou Institute of Chemical Physics, Chinese Academy of Sciences, Lanzhou 730000, P. R. China

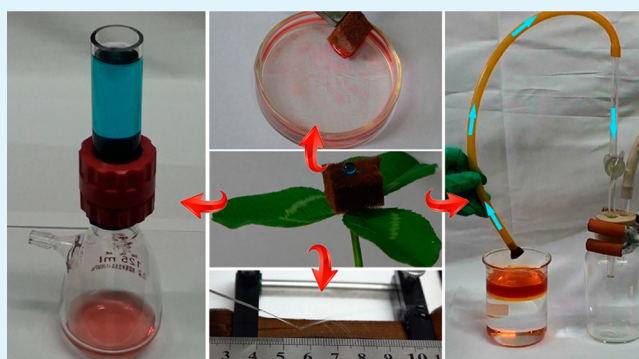
[‡]Center of Eco-material and Green Chemistry, Lanzhou Institute of Chemical Physics, Chinese Academy of Sciences, Lanzhou 730000, P. R. China

[§]Graduate University of the Chinese Academy of Sciences, Beijing 100049, P. R. China

S Supporting Information

ABSTRACT: Magnetic, durable, and superhydrophobic polyurethane (PU) sponges were fabricated by chemical vapor deposition (CVD) of tetraethoxysilane (TEOS) to bind the Fe₃O₄ nanoparticles tightly on the sponge and then dip-coating in a fluoropolymer (FP) aqueous solution. The sponges were characterized using scanning electron microscopy and other analytical techniques. The effects of CVD time of TEOS and FP concentration on wettability, mechanical properties, oil absorbency, and oil/water selectivity of the sponges were also investigated. The sponges exhibit fast magnetic responsivity and excellent superhydrophobicity/superoleophilicity ($CA_{\text{water}} = 157^\circ$ and $CA_{\text{oil}} \approx 0^\circ$). The sponges also show very high efficiency in oil/water separation and could, driven by a magnet, quickly absorb floating oils on the water surface and heavy oils under water. Moreover, the PU@Fe₃O₄@SiO₂@FP sponges could be used as membranes for oil/water separation and for continuous separation of large amounts of oil pollutants from the water surface with the help of a pump. The in turn binding of Fe₃O₄ nanoparticles, SiO₂, and FP can also improve mechanical properties of the PU sponge. The sponges maintain the superhydrophobicity even when they are stretched with 200% strain or compressed with 50% strain. The sponges also show excellent mechanical stability, oil stability, and reusability in terms of superhydrophobicity and oil absorbency. The magnetic, durable, and superhydrophobic PU sponges are very promising materials for practical oil absorption and oil/water separation.

KEYWORDS: superoleophilic, polyurethane sponges, silica, water purification, surface chemistry



INTRODUCTION

Materials for efficient oil absorption and oil/water separation have been in high demand since the oil spill disaster in the Gulf of Mexico. Many materials including polyurethane (PU) sponge, clay minerals, and nonwoven fabrics have been used to absorb oily compounds from water. However, most of the materials absorb both oil and water simultaneously, and their efficiency and selectivity in oil/water separation are low.¹ Wettability of the materials toward water and oil is one of the most important factors influencing their performance in selective oil absorption and oil/water separation. It is well-known that wettability of materials toward water and oil can be rationally controlled by chemical composition and geometrical structure of their surfaces.^{2,3}

Recently, superwetting materials, e.g., superhydrophobic/superoleophilic and underwater superoleophobic materials, have received much attention in the field of oil/water separation, and encouraging results have been obtained.^{4–9}

Superwetting materials including manganese nanowires^{10,11} and carbonaceous aerogels^{12–18} have been developed for oil/water separation. However, the toxic and expensive reagents and complicated and lengthy fabrication processes hamper their practical applications.^{15,16} Moreover, the efficient oil/water separation by superhydrophobic materials is owing to the superhydrophobic coatings, whereas most of the reported superhydrophobic materials are mechanically and chemically instable. On one hand, the micro/nanoscale roughness is essential in fabricating superhydrophobic surfaces but inherently weak toward mechanical abrasion. On the other hand, the materials with low surface energy for fabricating superhydrophobic surfaces are often chemically not stable toward acid, base, organic solvents, etc. The low stability of

Received: December 28, 2014

Accepted: February 11, 2015

Published: February 11, 2015

superhydrophobic materials is the bottleneck we are facing for their practical applications. Thus, simple methods for preparing durable superhydrophobic materials should be developed to meet their practical applications, e.g., oil/water separation.

Much effort has been made to prepare superwetting materials for oil/water separation via simple methods. Superwetting papers,¹⁹ metal meshes,^{20–24} and fabrics^{1,9} have been reported for efficient oil/water separation. Unfortunately, the absorbency of these filmwise materials for oil is very low.²⁵ Different from these filmwise materials, porous sponges and aerogels with three-dimensional architecture can not only achieve oil/water separation but also absorb a large volume of oil. Commercially available PU sponges with high porosity, large surface area, low density, and good elasticity are excellent substrates for preparing superwetting materials for oil/water separation and oil absorption.^{8,26–32} However, PU sponges absorb water and oil simultaneously, which makes them impractical to be used directly for selective removal of oils from water. Therefore, researchers have tried various methods, e.g., increasing the surface roughness and decreasing the surface tension, to prepare superhydrophobic PU sponges for efficient oil/water separation. In most cases, the activation of PU sponges with sulfuric acid, dichromic acid, or SnCl₂ is a necessary step.^{8,26–29} The activation of PU sponges not only forms a micro/nanoscale hierarchical structure on the surface but also generates hydrophilic groups, such as –OH and –COOH,^{8,27–29} which makes it possible for further modification of PU sponges. The surface etching of PU sponges is of benefit for making them superhydrophobic but inevitably sacrifices their mechanical properties compared to the pristine counterpart. Moreover, the acidic wastes in the activation process will result in secondary pollution. Therefore, it is necessary to find a facile and green strategy for fabricating superhydrophobic PU sponges.

Alternatively, magnetic superhydrophobic/superoleophilic particles can be placed on the polluted water zone and subsequently be removed by an external magnetic field, which arouse great interests for preparing magnetic oil absorbents.^{33–36} However, the good mobility and dispersibility of superhydrophobic particles on the water surface prohibit their large-scale application. Immobilization of magnetic particles on porous sponges to form magnetic and superhydrophobic sponges is an effective approach to overcome the problems.^{37,38} Tight binding of magnetic particles onto the sponges is essential in order to avoid falloff of the particles and to keep the magnetic property.³⁹

Here we report a facile approach for preparing magnetic, durable, and superhydrophobic PU sponges on the basis of our previous work on durable superhydrophobic surfaces.^{40,41} The superhydrophobic PU sponges feature fast magnetic responsiveness, excellent superhydrophobicity/superoleophilicity, high mechanical and chemical stabilities, as well as high oil/water separation efficiency and oil absorbency. The reusable superhydrophobic PU sponges can, driven by a magnet, selectively absorb floating oils on the water surface and heavy oils under water and even achieve continuous oil/water separation with the help of a vacuum pump.

■ EXPERIMENTAL SECTION

Materials. Commercial PU sponges were supplied by Shaoxing Chenfeng Foam Co. Ltd., Zhejiang, China. Tetraethoxysilane (TEOS, 99.9%) was purchased from Gelest. Trisodium citrate dihydrate, FeCl₃·6H₂O, FeSO₄·7H₂O, K₂Cr₂O₇, acetone, chloroform, 1, 2-dichloro-

obenzene, ethanol, tetrachloromethane, petroleum ether, toluene, *n*-hexane, H₂SO₄, NaOH, ammonia (25 wt %), methylene blue (MB), Sudan Red I, and Oil Red O were purchased from China National Medicines Co. Ltd. Commercial petrol and crude oil were purchased from Sinopec, Lanzhou, China. Soybean oil was bought from a local supermarket, Lanzhou, China. Fluoropolymer (FP) emulsion containing 25 wt % FP, water, and propylene glycol was provided by 3 M Co. Ltd. (Scotchgard PM-3633). All chemicals were used as received without further purification. Deionized water was used for all experiments and tests.

Preparation of Fe₃O₄ Nanoparticles (NPs). The magnetic Fe₃O₄ NPs were prepared by the coprecipitation method.^{42,43} Briefly, 50 mL of 25 wt % ammonia was added into the aqueous solution containing 18 g of FeSO₄·7H₂O and 26 g of FeCl₃·6H₂O in a N₂ atmosphere under vigorous mechanical stirring. Then, 7.5 g of trisodium citrate dihydrate was added to the mixture and stirred for 1 h at 70 °C. The mixture was repeatedly separated by a magnet and washed with deionized water and ethanol.

Preparation of Magnetic, Durable, and Superhydrophobic PU@Fe₃O₄@SiO₂@FP Sponges. First, PU sponges (1 × 1 × 1 cm or 1 × 1 × 6 cm) were washed in turn with deionized water and ethanol for several times and then dried in an oven at 60 °C. A piece of the cleaned PU sponge was immersed in 5 mL of acetone containing 30 mg of the homogeneously dispersed Fe₃O₄ NPs and sonicated for 30 min at 30 °C. The PU@Fe₃O₄ sponge was annealed at 110 °C for 30 min to remove acetone and then put in a vacuum desiccator containing 4 mL of ammonia (25 wt %) and 4 mL of TEOS. After chemical vapor deposition (CVD) of TEOS for a period of time (0, 4, 12, 24, and 48 h), the as-prepared PU@Fe₃O₄@SiO₂ sponges were immersed in 4 mL of FP solutions of different concentrations (0%, 1%, 2.5%, 5%, and 10%) and sonicated at 30 °C for 30 min. Finally, the PU@Fe₃O₄@SiO₂@FP sponges were annealed at 110 °C for 15 min.

Measurement of Water Shedding Angle (WSA). Owing to the fact that the surfaces of some substrates such as textiles and sponges are macroscopically rough, it is very difficult to detect the full drop profile for contact angle (CA) measurement (Supporting Information (SI), Figure S1). Consequently, the classical CA measurement, highly dependent on the method of drop shape analysis, is unsuited to reliably evaluate the wetting properties of the superhydrophobic sponges. Thus, WSA is used instead of CA and sliding angle (SI, Figure S2).^{44,45} Typically, the sample was fixed onto a glass slide and placed on the tilting table of the Contact Angle System OCA 20 (Dataphysics, Germany). A syringe was mounted above the tilting table with a fixed needle to a substrate distance of 10 mm. The syringe was positioned in a way that a drop falling from the needle would contact the substrate 8 mm from the bottom end of the sample. The needle with an inner diameter of 110 μm was used to produce liquid drops of 7 ± 0.3 μL. To determine the WSA, measurements were started at an inclination angle of 50°. Water drops were released onto the sample at a minimum of three different positions. If all drops completely bounced or rolled down the sample, the inclination angle was reduced by 2° and the procedure repeated until one or more of the droplets would not completely roll down the surface. The lowest inclination angle at which all the drops completely rolled down or bounced off the surface was noted as the WSA.

Oil Absorbency. A piece of sample was immersed in oil at room temperature. The sample was taken out of the oil after 1 min, drained for several seconds, and wiped with filter paper to remove excess oil. The oil absorbency *k* of the sample was determined by weighing the sample before and after oil absorption and calculated according to the following equation:

$$k = (m_t - m_i) / m_i$$

where *m_t* is the weight of the wet sample with oil (g) and *m_i* is the weight of the dry sample (g).

Stability in Oils and Reusability. For the stability in oils tests, a piece of sample was immersed in petrol, toluene, and chloroform for 1, 24, and 168 h. Afterward, the sample was washed with *n*-hexane and dried in an oven at 60 °C before WSA measurement. For the reusability tests, a piece of sample was immersed in 20 mL of petrol,

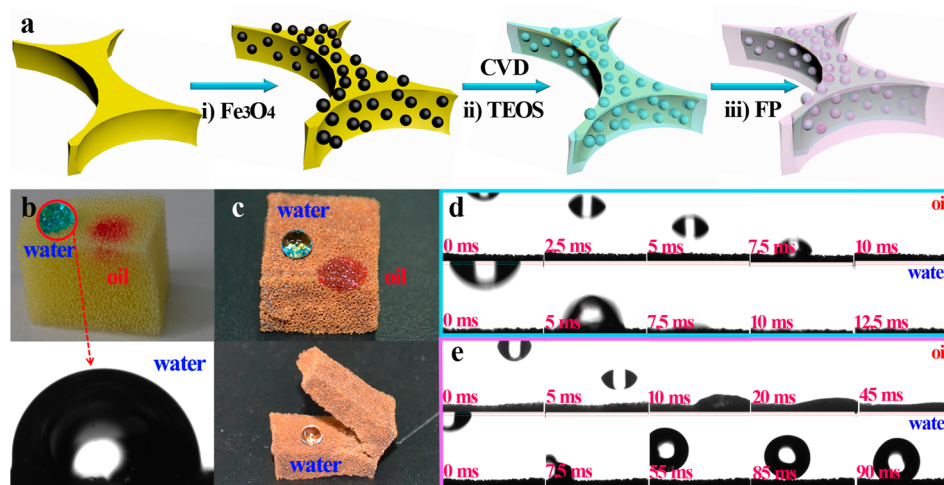


Figure 1. (a) Schematic illustration for preparing the PU@Fe₃O₄@SiO₂@FP sponges, (b) images of the pristine PU sponge partly wetted by water and completely wetted by oil, (c) images of the surface and the cross section of the PU@Fe₃O₄@SiO₂@FP sponge with spherical water drops on it but completely wetted by oil, the snapshots of dropping water and oil on the (d) PU@Fe₃O₄@SiO₂ and (e) PU@Fe₃O₄@SiO₂@FP (CVD of TEOS for 24 h, 5% FP solution) sponges taken using Contact Angle System OCA 20. Water was colored with MB, and oil was colored with Oil Red O.

toluene, and chloroform for 1 min to reach equilibrium and then taken out and squeezed by hand to remove the absorbed oils. The sample was washed with *n*-hexane to remove the residual oils and dried in an oven at 60 °C. This absorption–desorption procedure was repeated 10 times. After each cycle, the WSA and oil absorbency were measured.

Characterization. The micrographs of samples were taken using a field emission scanning electron microscope (SEM, JSM-6701F, JEOL). Before SEM observation, all samples were fixed on aluminum stubs and coated with gold (~7 nm). X-ray photoelectron spectra (XPS) were obtained using a VG ESCALAB 250 Xi spectrometer equipped with a Monochromated Al K α X-ray radiation source and a hemispherical electron analyzer. The spectra were recorded in the constant pass energy mode with a value of 100 eV, and all binding energies were calibrated using the C 1s peak at 284.6 eV as the reference. To study the dynamic interaction of sponges with water and oil drops, high speed videos were recorded at 400 fps using the Contact Angle System OCA 20. The mechanical properties of sponges (1 × 1 × 6 cm) were measured using a universal testing machine (CMT4304, Shenzhen SANS Test Machine Co. Ltd., Shenzhen, China) equipped with a 200 N load cell at room temperature. The tests were performed with a gauge length of 3 cm and a loading speed of 10 cm/min. The water contents in commercial petrol and recovered petrol from water were measured using a Mettler Toledo C20 coulometric Karl Fisher titrator. All the tests were carried out in triplicate, and the average values were presented.

RESULTS AND DISCUSSION

Fabrication of PU@Fe₃O₄@SiO₂@FP Sponges. The PU@Fe₃O₄@SiO₂@FP sponges were prepared according to the procedure as shown in Figure 1a. Once immersed in a homogeneous dispersion of Fe₃O₄ NPs in acetone, the PU sponge quickly absorbed acetone and Fe₃O₄ NPs simultaneously. After heated in an oven to remove acetone, the Fe₃O₄ NPs were attached on the surface of the PU skeleton and the PU@Fe₃O₄ sponge was formed. The PU sponge was uniformly coated with the Fe₃O₄ NPs, but the interaction between them was weak. Deformation of the PU@Fe₃O₄ sponge resulted in falling off of the Fe₃O₄ NPs (Figure S3a). Also, a lot of Fe₃O₄ NPs fell off the PU@Fe₃O₄ sponge once immersed in water (Figure S3b). Thus, the PU@Fe₃O₄ sponge was subsequently coated with a thin layer of SiO₂ via CVD of TEOS according to a previously reported method.⁴⁶ The SiO₂ layer binds the Fe₃O₄ NPs tightly on the surface of the PU skeleton. No falling

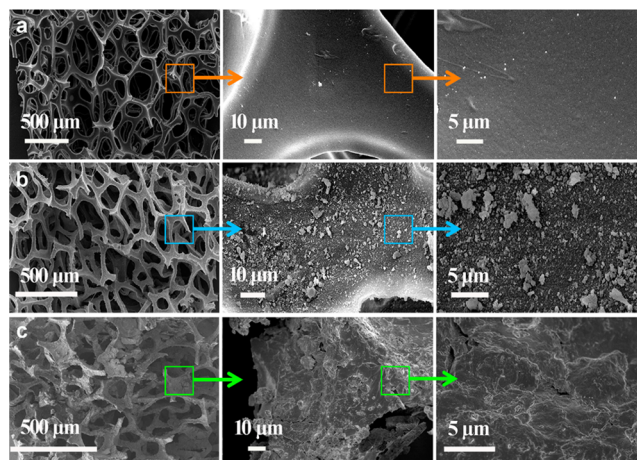


Figure 2. SEM images of (a) PU, (b) PU@Fe₃O₄@SiO₂, and (c) PU@Fe₃O₄@SiO₂@FP (CVD of TEOS for 24 h, 5% FP solution) sponges.

of the Fe₃O₄ NPs was observed after large and repeated deformation of the PU@Fe₃O₄@SiO₂ sponge or immersed in water. Finally, the PU@Fe₃O₄@SiO₂ sponge was dip-coated in an FP aqueous solution and then annealed in an oven to form the magnetic, durable, and superhydrophobic PU@Fe₃O₄@SiO₂@FP sponge. The density of the PU sponge increased from 36.9 to 40.9 mg/cm³ after incorporation of Fe₃O₄ NPs and deposition of SiO₂ and then further increased to 85.9 mg/cm³ after modified with FP.

Evident changes in wettability of the PU sponge occurred in the process of preparing the PU@Fe₃O₄@SiO₂@FP sponge (Figure 1b–e and SI, Movie S1). The pristine PU sponge can be easily wetted by both water and oil (Figure 1b). Oil drops penetrated into the PU sponge in 5 ms, whereas the CA_{water} decreased gradually when a water drop was loaded on the PU sponge. The CA_{water} decreased to 87° after dropped on the surface of the PU sponge for 1 min. The PU sponge became superamphiphilic after in turn introduction of the Fe₃O₄ NPs and the SiO₂ layer. Water and oil drops needed 7.5 and 2.5 ms, respectively, to completely penetrate into the PU@Fe₃O₄@SiO₂ sponge (Figure 1d). The further modification of the PU@

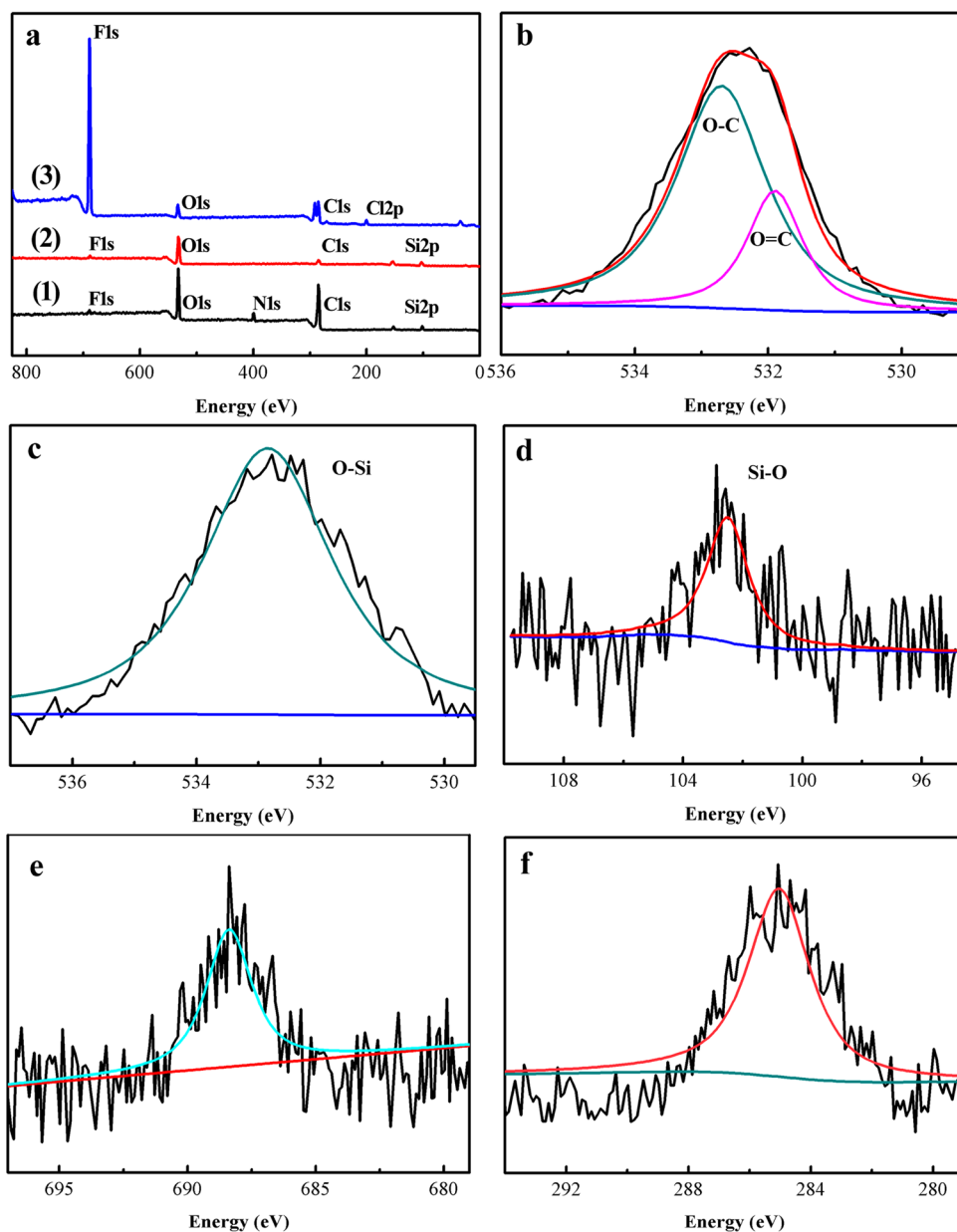


Figure 3. (a) XPS spectra of (1) PU, (2) PU@Fe₃O₄@SiO₂, and (3) PU@Fe₃O₄@SiO₂@FP (CVD of TEOS for 24 h, 5% FP solution), (b) O 1s peak fitting of PU, (c) O 1s and (d) Si 2p peak fitting of PU@Fe₃O₄@SiO₂, and (e) F 1s and (f) Cl 2p peak fitting of PU@Fe₃O₄@SiO₂@FP sponges.

Fe₃O₄@SiO₂ sponge with FP generated the superhydrophobic/superoleophilic PU@Fe₃O₄@SiO₂@FP sponge. Water drops showed very high CA on the PU@Fe₃O₄@SiO₂@FP sponge. However, it is impossible to get the accurate outline of water drops (dash line in SI, Figure S1) and then measure the CA and CA hysteresis exactly because the sponge surface is macroscopically rough, pliant and nonreflective.^{44,45} Thus, WSA was used to evaluate water repellent properties of the sponge instead of CA and CA hysteresis as mentioned in the Experimental Section. Water drops on both the surface and the cross section are spherical in shape, indicating uniformity of the superhydrophobic coating (Figure 1c). Water drops are in the Cassie–Baxter state on the PU@Fe₃O₄@SiO₂@FP sponge since the CA is very high, and the WSA is 2–3° and water drops could easily roll off the slightly tilted sample. In addition, water drops released from a height of 10 mm could bounce off

the surface of the sponge easily. In spite of excellent water repellent property, the PU@Fe₃O₄@SiO₂@FP sponge can be easily wetted by oils. Drops of petrol could completely penetrate into the sample in 35 ms (Figure 1e).

The surface morphology of PU, PU@Fe₃O₄@SiO₂, and PU@Fe₃O₄@SiO₂@FP sponges are shown in Figure 2. The pristine PU sponge is composed of many interconnected micropores with a diameter of 200–400 μm (Figure 2a). The wall of the micropores with a thickness of ~50 μm is very smooth. The surface became very rough after modification with Fe₃O₄ NPs. The SiO₂ layer generated by CVD of TEOS is about 20 nm in thickness.⁴⁶ The SiO₂ layer is linked to the surface of the Fe₃O₄ NPs via the Fe–O–Si bond.^{47–51} The surface of the PU@Fe₃O₄@SiO₂ sponge shows hierarchical micro/nanoscale roughness (Figure 2b). The SEM images of the PU@Fe₃O₄@SiO₂@FP sponge reveals that FP is deposited

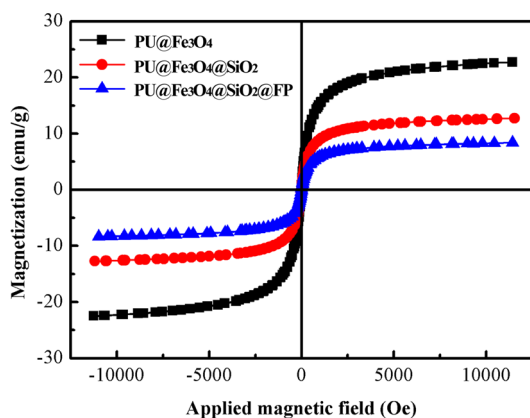


Figure 4. Magnetic curves (300 K) of PU@Fe₃O₄, PU@Fe₃O₄@SiO₂, and PU@Fe₃O₄@SiO₂@FP (CVD of TEOS for 24 h, 5% FP solution) sponges.

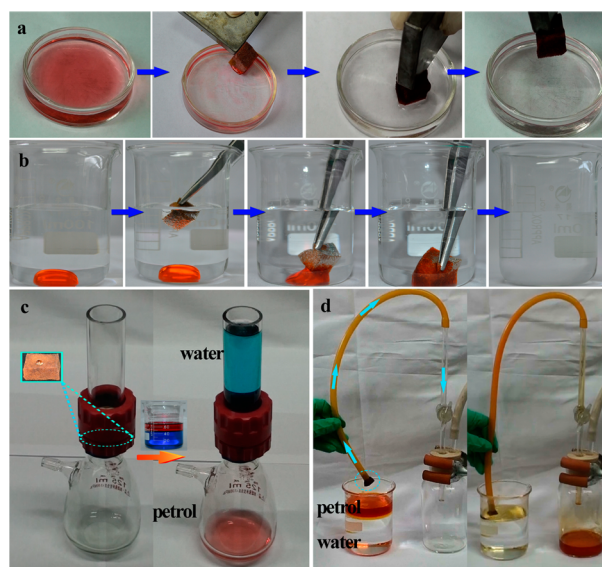


Figure 5. Absorption of (a) floating petrol on water surface and (b) chloroform under water, (c) oil/water separation, and (d) pump assisted continuous separation of floating petrol on water surface using PU@Fe₃O₄@SiO₂@FP sponges (CVD of TEOS for 24 h, 5% FP solution). Petrol, chloroform, and water were colored with Oil Red O, Sudan Red I, and MB, respectively.

uniformly over the whole framework in the dip-coating step (Figure 2c). The FP layer not only makes the PU@Fe₃O₄@SiO₂ sponge superhydrophobic but also is helpful to further immobilize the Fe₃O₄ NPs. The PU@Fe₃O₄@SiO₂@FP sponge shows a 3D interconnected porous network with a hierarchical rough surface. None of the pores inside the PU@Fe₃O₄@SiO₂ sponge is blocked, which is of benefit for the fast uptake of oils.¹³

The surface chemical composition of PU, PU@Fe₃O₄@SiO₂, and PU@Fe₃O₄@SiO₂@FP sponges were analyzed by XPS (Figure 3a). The C 1s (284 eV), N 1s (399 eV), and O 1s (532 eV) peaks can be seen clearly in the spectrum of the PU sponge. In addition, the weak Si 2s (153 eV), Si 2p (101 eV), and F 1s (687 eV) peaks are also detectable, indicating that the PU sponge is modified with a compound containing Si and F elements. There are signals at 531.6 (C=O) and 532.8 eV (C–O) in the O 1s spectrum of PU (Figure 3b).⁵² After introduction of the Fe₃O₄ NPs and the SiO₂ layer, the C 1s

peak becomes very weak and the N 1s peak even disappears, whereas the Si 2s and Si 2p peaks become strong as shown in the spectrum of the PU@Fe₃O₄@SiO₂ sponge. The O 1s (532.9 eV) and Si 2p (102.5 eV) peaks (Figure 3c,d) prove the formation of the SiO₂ layer on the surface of the PU@Fe₃O₄ sponge.^{53,54} The differences in the O 1s peak between PU and PU@Fe₃O₄@SiO₂ sponges confirmed that the PU@Fe₃O₄ sponge was covered with a layer of SiO₂. In addition, no peak corresponding to the Fe element was detected. As is well-known, the XPS analysis provides surface chemical composition with a detecting depth of a few nanometers. The weakened C 1s peak, the disappeared N 1s peak, and the absence of the Fe peak mean that the PU@Fe₃O₄ sponge is well coated with a layer of SiO₂. After further coated with FP, a very strong F 1s (688.4 eV) peak and weak Cl 2p (200.6 eV) peak were detected in the spectrum of the PU@Fe₃O₄@SiO₂@FP sponge (Figure 3e,f).⁵⁵ Meanwhile the Si 2s and Si 2p peaks disappear, and the O 1s peak becomes very weak. The combination of such a surface chemical composition and micro/nanoscale roughness endow the PU@Fe₃O₄@SiO₂@FP sponge with excellent water repellent property.

The magnetic property of the sponges after stepwise modification was examined and compared with that of the Fe₃O₄ NPs (Figures 4 and S4 in the SI). All the samples show standard paramagnetic characteristic curves with no hysteresis after removal of the magnetic field. The PU sponge became magnetic with a saturation magnetization of 22.73 emu/g after incorporation of the Fe₃O₄ NPs (62.21 emu/g). The saturation magnetization decreased to 12.72 emu/g for the PU@Fe₃O₄@SiO₂ sponge and then to 8.37 emu/g for the PU@Fe₃O₄@SiO₂@FP sponge. The decrease in the saturation magnetization after stepwise modification of the PU sponge is reasonable. Similar results have been reported by other researchers.⁵⁶ The PU@Fe₃O₄@SiO₂@FP sponge can be easily manipulated using a magnet.

Selective Oil/Water Separation. The superhydrophobic/superoleophilic property of the PU@Fe₃O₄@SiO₂@FP sponge endows it with high selectivity for oil/water separation. In addition, the porous and interconnected skeleton of the sponge provides a large volume for the storage of oils. The sponge can be magnetically driven to the polluted water zone using a magnet as shown in Figure 5a and SI, Movie S2. The oil is quickly absorbed within a few seconds when the superhydrophobic sponge contacts it. The oil-loaded sponge remains floating on the water surface and can be magnetically manipulated after complete removal of oil from water. The magnetic responsiveness of the superhydrophobic sponge provides a new approach for handling after oil absorption. The sponge can also be used to absorb heavy oils under water (Figure 5b). When the sponge is immersed in water by an external force, it is reflective because of the existence of the air cushion between water and the sponge. Most of the area between them is the liquid/vapor interface and the ratio of liquid/solid interface is pretty small, which indicates that the interaction between water and the superhydrophobic sponge is very weak. Once the sponge contacted the chloroform under water, the chloroform could be quickly absorbed within a few seconds. Subsequently, the absorbed oil can be entirely removed from the mixture by taking the sponge out of water, suggesting that the sponge is also useful for cleaning oils under water.

The PU@Fe₃O₄@SiO₂@FP sponge can also be used as a membrane for oil/water separation (Figure 5c and SI, Movie S3). The sponge was fixed between a glass tube with an inner

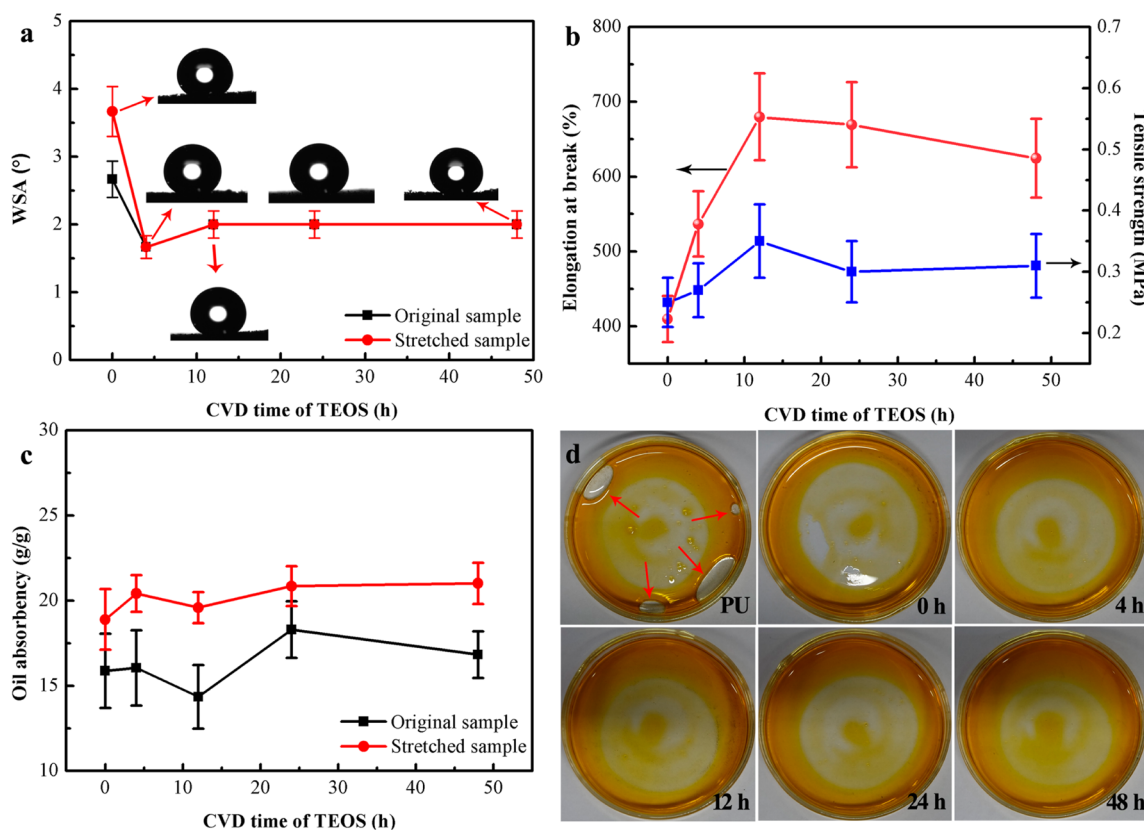


Figure 6. Effects of CVD time of TEOS on (a) WSAs, (b) mechanical properties, (c) absorbency for petrol, and (d) oil/water selectivity of the PU@Fe₃O₄@SiO₂@FP sponges (5% FP solution).

diameter of 25 mm and a flask. A mixture of 20 mL of oil colored with Oil Red O and 50 mL of water colored with MB was poured slowly onto the glass tube. Once poured into the custom built setup, oils with high density will sink to the bottom and be absorbed by the sponge or penetrate the sponge. Oils with low density contact the sponge before water when the mixture is slowly pulled into the custom built setup because of their lower density than water. The oil quickly penetrates through the sponge and drops into the bottle beneath it. Meanwhile, more and more water is collected on the surface of the sponge.

The oil absorbency of most of the reported superhydrophobic materials is about tens of their own weight. After absorption equilibrium, the absorbed oil must be collected or removed from the materials in order to be used for the next cycle. For expanding their practical applicability in the continuous collecting of large amounts of oil pollutants from water, the PU@Fe₃O₄@SiO₂@FP sponge was fixed at the opening of a tube and combined with an external pump (Figure 5d and SI, Movie S4). Once the sponge was placed at the oil/water interface, a part of the floating petrol was quickly absorbed by the sponge, but no water was absorbed because the sponge is superoleophilic and superhydrophobic. However, there is much excess oil remained on water surface owing to the fact that the sponge is not big enough to absorb all the oil on the water surface. Once the pump was started, the absorbed oil in the sponge can be pumped into the collector through the tube and the released the space in the sponge can absorb the excess oil on water surface. Thus, the absorption and collection of oil can be achieved simultaneously and continuously. All the petrol on water surface could be collected successfully using a

small piece of the PU@Fe₃O₄@SiO₂@FP sponge with the help of the pump. No water can be seen in the collected oil. The water concentration in the collected petrol is 246.2 ppm, which is comparable to that in the original petrol (252.7 ppm), implying very high oil/water separation efficiency.

Effects of CVD Time of TEOS and FP Concentration on Wettability, Mechanical Properties, Oil Absorbency and Oil/Water Selectivity. The effects of CVD time of TEOS on WSAs, mechanical properties, oil absorbency, and oil/water selectivity are shown in Figure 6. The WSA slightly decreased after CVD of TEOS, and the increase in CVD time had no influence on WSA (Figure 6a). The broken samples by stretching show almost the same WSAs as the original samples regardless of the CVD time. With increasing the CVD time from 0 to 12–24 h, the elongation at break increases from 409.68% to 679.66~669.3% (Figure 6b). The further increase in the CVD time to 48 h results in a slight decrease of the elongation at break to 624.47%. Similar tendency of the tensile strength was observed with increasing the CVD time (Figure 6b). The tensile strength is as high as 0.35 MPa when the CVD time is 12 h. The absorbency of the sponges for petrol was slightly improved with increasing the CVD times to 24 h (Figure 6c). The oil absorbency of broken samples by stretching is higher than that of original ones. Mechanical deformation such as stretching could enlarge the pores of the sponge, which is beneficial for storage of more oil. The oil/water selectivity of the PU sponge is low. The absorbed liquids in the sponges were collected by hand squeezing (Figure 6d). The PU sponge simultaneously absorbs oil and water (indicated by arrows), while CVD time of TEOS has no

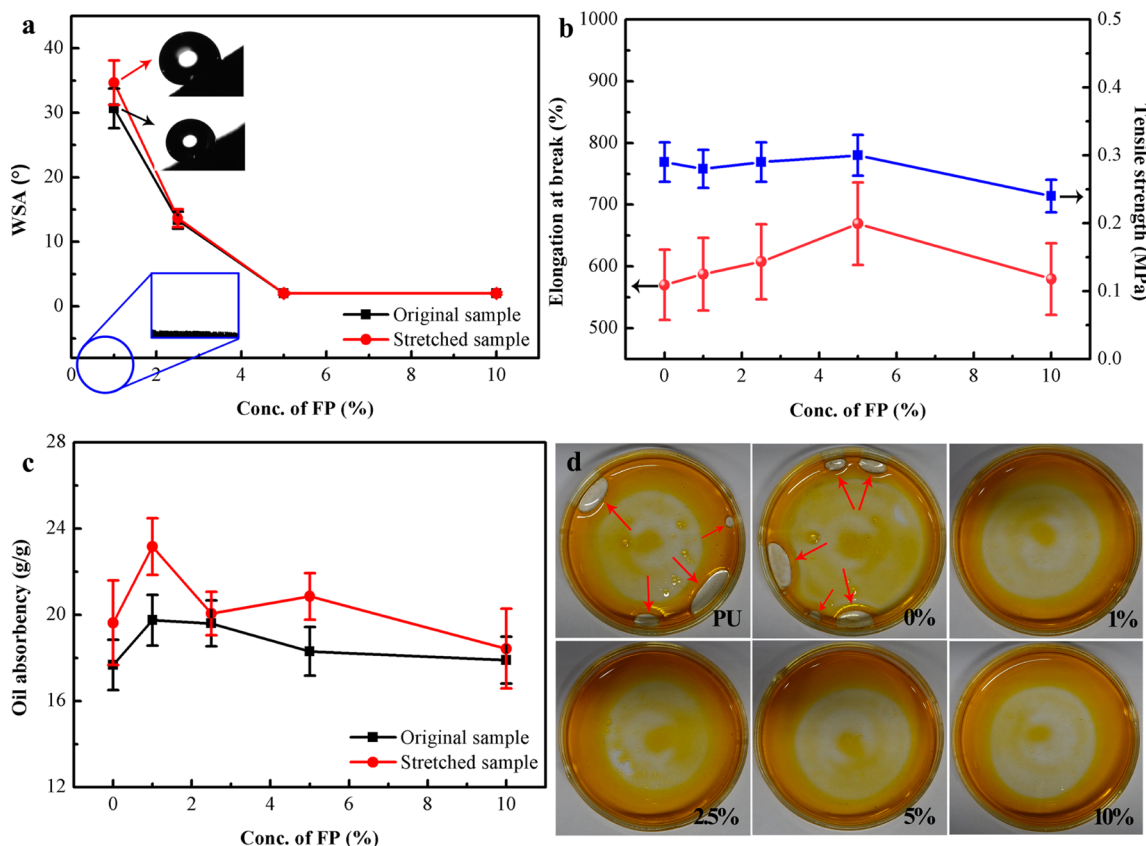


Figure 7. Effects of FP concentration on (a) WSAs, (b) mechanical properties, (c) absorbency for petrol, and (d) oil/water selectivity of the PU@Fe₃O₄@SiO₂@FP sponges (CVD of TEOS for 24 h).

Table 1. Mechanical Properties of PU, Chromic Acid Etched PU, and PU@Fe₃O₄@SiO₂@FP (CVD of TEOS for 24 h, 5% FP Solution) Sponges

samples	tensile strength/MPa	elongation at break/%
pristine	0.30	548
etched	0.32	344.5
PU@Fe ₃ O ₄ @SiO ₂ @FP	0.33	669.3

obvious effect on oil/water selectivity and all samples show high oil/water selectivity.

FP concentration has great influences on WSAs, mechanical properties, oil absorbency, and oil/water selectivity of the PU@Fe₃O₄@SiO₂@FP sponge (Figure 7). FP plays an important role in lowering surface energy of the sponge to achieve superhydrophobicity. Without FP, the PU@Fe₃O₄@SiO₂ sponge is hydrophilic (blue rectangle in Figure 7a). The sponge becomes superhydrophobic (WSA = 30.7°) when the FP concentration is 1%. The WSA decreases sharply with increasing the FP concentration to 5%. The further increase in FP concentration to 10% has no influence on WSA. Breaking of the samples by stretching has no influence on WSA. The elongation at break increases from 570.0% to 669.3% with increasing the FP concentration from 0% to 5% and then decreases to 579.7% with further increasing the concentration to 10% (Figure 7b). Similar tendency of the tensile strength was observed with increasing the FP concentration. A FP concentration of 5% is of benefit to the WSA and the mechanical properties. Oil absorbency of the PU@Fe₃O₄@SiO₂@FP sponge is higher than that of the uncoated one but slightly decreases with increasing the FP concentration (Figure

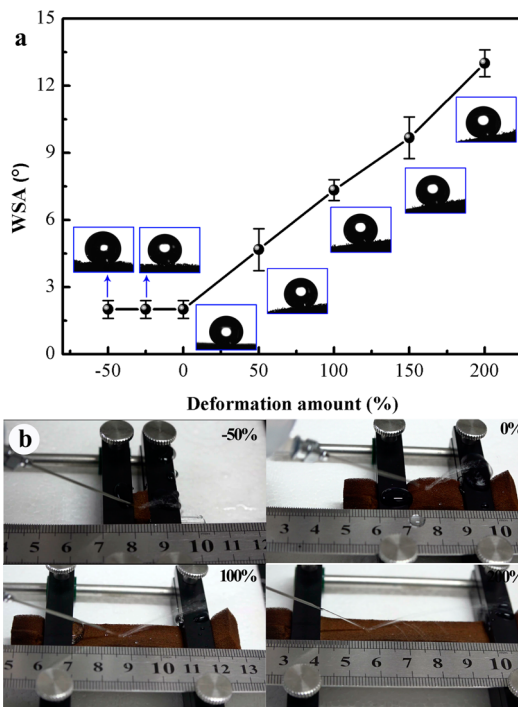


Figure 8. Effects of deformation degree of the PU@Fe₃O₄@SiO₂@FP (CVD of TEOS for 24 h, 5% FP solution) sponges on (a) WSA and (b) water jet bounce behavior.

7c). Oil absorbency of broken samples by stretching is higher than that of the original ones. The PU@Fe₃O₄@SiO₂ sponge

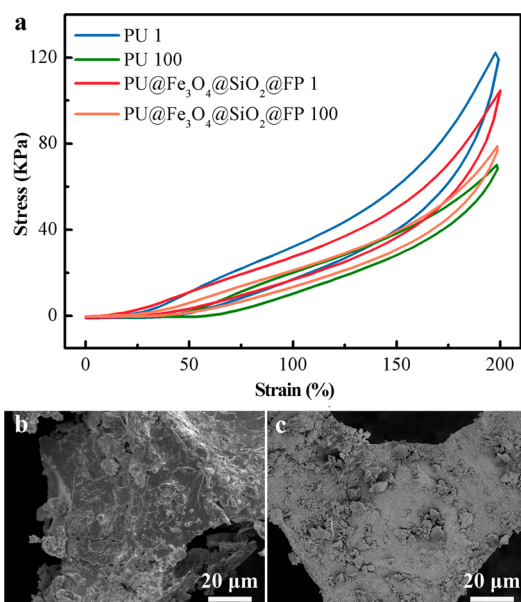


Figure 9. (a) Representative cyclic compressive stress–strain curves of the PU and PU@Fe₃O₄@SiO₂@FP (CVD of TEOS for 24 h, 5% FP solution) sponges in 100 cycles of successive 200% strain tests and SEM images of the PU@Fe₃O₄@SiO₂@FP sponge (b) before and (c) after 100 cycles of successive 200% strain.

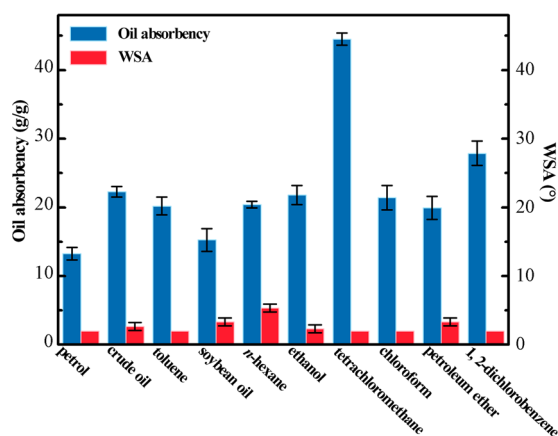


Figure 10. Oil absorbency of the PU@Fe₃O₄@SiO₂@FP (CVD of TEOS for 24 h, 5% FP solution) sponges for different oils and the WSAs after they have been used once for oil absorption.

simultaneously absorbs oil and water (arrows in Figure 7d). While all the FP-coated samples only absorb oil.

Mechanical Stability. Pretreatment of PU sponges using oxidative solutions, e.g., H₂SO₄/CrO₃, is frequently used to form micro/nanoscale hierarchical structures and to make the surface hydrophilic for further modification.^{26–29} Of primary importance to a coating is that it does not affect mechanical properties of the substrate, e.g., tensile strength and flexibility. No evident change in the tensile strength of the PU sponge was detected after treatment in 0.083 M chromic acid solution for 1 min (Table 1). However, the elongation at break decreases from 548% to 344.5%. Besides the sacrifice of the mechanical properties, the acidic wastes produced by etching of PU sponges undoubtedly result in secondary pollution. The pollutive, time-consuming, and lengthy procedures for preparing superhydrophobic PU sponges seriously restrict their practical applications. Instead, the mild and environ-

mentally friendly approach reported herein not only makes the PU sponges superhydrophobic but also enhances the elongation at break.

The effect of compression and stretching of the PU@Fe₃O₄@SiO₂@FP sponges on their wettability is presented in Figure 8 and SI, Movie S5. The WSA of the PU@Fe₃O₄@SiO₂@FP sponge is 2°, and compression by 25% and 50% has no influence on the WSA (Figure 8a). The WSA increases linearly from 2° to 14° with increasing the strain of the sponge from 0 to 200%. Water drops could easily roll off the 15° tilted samples. A jet of water could bounce off all the deformed PU@Fe₃O₄@SiO₂@FP sponge without leaving a trace regardless of the deformation degree (Figure 8b and SI, Movie S5), indicating excellent superhydrophobicity of the highly deformed samples. In the SI, Movie S6, a 7 μL water droplet was released to the surface of the sample with a strain of 200%. The sample was slowly moved in vertical and horizontal directions to show the liquid/solid interaction of the PU@Fe₃O₄@SiO₂@FP sponge with an extremely large deformation. No observable deformation of the water droplet could be detected while moving the porous sample vertically and horizontally, which indicates that the interaction between water and the surface is very weak.

The representative cyclic compressive stress–strain curves of the PU and PU@Fe₃O₄@SiO₂@FP sponges in 100 cycles of successive 200% strain tests are shown in Figure 9a. The stress of the PU and PU@Fe₃O₄@SiO₂@FP sponges at 200% strain in the first cycle is 122.24 and 104.74 KPa, respectively. The stress of the PU sponge at 200% strain decreases to 70.15 KPa (42.6% decline) after 100 cycles of the cyclic compression tests, whereas that of the PU@Fe₃O₄@SiO₂@FP sponge is 78.93 KPa (24.6% decline). This means high mechanical stability of the PU@Fe₃O₄@SiO₂@FP sponge. No change in WSA was recorded after 100 cycles of successive 200% strain. The SEM observation indicates that the 3D porous network of the PU@Fe₃O₄@SiO₂@FP sponge with a hierarchical rough surface remained unchanged after 100 cycles of successive 200% strain (Figure 9b,c).

Oil Absorbency and Stability in Oils. Ten kinds of frequently encountered organic liquids in daily life and industry, fuels (petrol and crude oil), food oils (soybean oil), alkane (*n*-hexane), chloroalkanes (chloroform and tetrachloromethane), alcohol (ethanol), ether (petroleum ether), and aromatic compounds (toluene and 1, 2-dichlorobenzene), were used to evaluate the absorbency of the PU@Fe₃O₄@SiO₂@FP sponges. The sponges show high absorbency for these organics (Figure 10). In general, the absorbency of the sponge for these organics is in the range of 13.26–44.50 g/g. No dripping of the absorbed oil was observed in the handling process indicating firm absorption by the sponges. The oil absorbency of the PU@Fe₃O₄@SiO₂@FP sponge depends mainly on the density of the organics. For example, the absorbency of the sponge for tetrachloromethane (density = 1.60 g/cm³) is 44.50 g/g, but for *n*-hexane (density = 0.66 g/cm³) is 20.42 g/g. The surface tension and viscosity of the organics also have some influences on oil absorbency of the sponge as shown in SI, Table S1. In addition, the WSA of the sponge after it was used for oil absorption for one time is in the range of 2–6.3° regardless of the kind of oil, which is comparable to the freshly coated sample (WSA = 2–3°). This result indicates that the PU@Fe₃O₄@SiO₂@FP sponges still retain excellent superhydrophobicity after absorption of various oils. The oil absorbency of the PU@Fe₃O₄@SiO₂@FP sponge is comparable with those

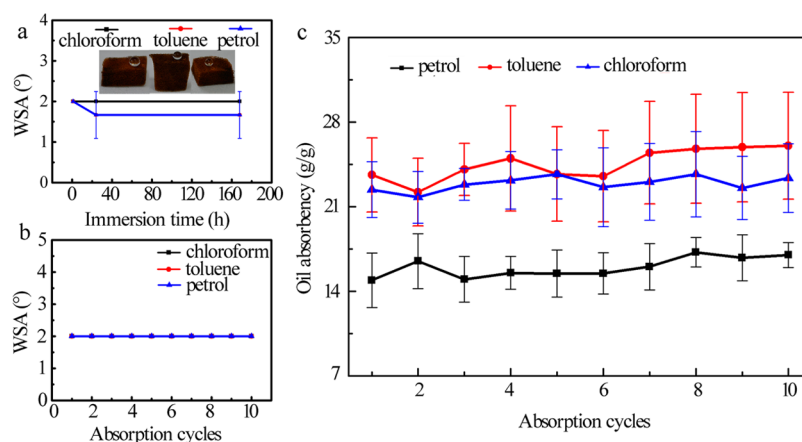


Figure 11. (a) Variation of WSAs of the PU@Fe₃O₄@SiO₂@FP (CVD of TEOS for 24 h, 5% FP solution) sponges with immersion time in chloroform, toluene, and petrol and the corresponding images of the sponges with water drops after immersion in oils for 168 h, variation of (b) WSAs and (c) oil absorbency of the PU@Fe₃O₄@SiO₂@FP sponges with absorption cycles for chloroform, petrol, and toluene.

previously reported (SI, Table S2),^{8,26,27,30,57,58} but the remarkable superiority of the PU@Fe₃O₄@SiO₂@FP sponge in facile preparation, magnetic responsivity, and excellent mechanical and chemical stability make them very promising materials for practical oil absorption and oil/water separation.

The efficient oil/water separation of superhydrophobic materials is owing to the superhydrophobic coatings, whereas most of the reported superhydrophobic coatings are mechanically and chemically instable.⁴⁰ An obvious decrease in the water CA to 136° was observed after five absorption cycles for the superhydrophobic PU sponge.⁵⁸ Excellent mechanical and chemical stability of superhydrophobic PU sponges are essential for their practical application in oil/water separation. The PU@Fe₃O₄@SiO₂@FP sponges show excellent long time stability in chloroform, toluene, and petrol in terms of superhydrophobicity (Figure 11a). The influence of long time immersion in solvents on superhydrophobicity of the samples is negligible. The WSA remained in the range of 1.5–2.0° after kept in chloroform, toluene, and petrol for 168 h. Water drops are spherical in shape and could easily roll off the samples after the stability test in solvents as shown in the insets in Figure 11a.

Chloroform, petrol, and toluene were chosen to evaluate the reusability of the PU@Fe₃O₄@SiO₂@FP sponge (Figure 11b,c). The absorbencies of the sponge for chloroform, petrol, and toluene are 22.4, 14.9, and 23.6 g/g, respectively, in the first cycle. The absorbent can be easily recycled using a magnet even after repeatedly used for ten times as shown in SI, Figures S5 and S6 and Movie S7. The increase in the absorption cycles has no obvious influence on the oil absorbency. The WSAs are 2° regardless of absorption cycles and kinds of oils. The excellent reusability of the PU@Fe₃O₄@SiO₂@FP sponge in terms of oil absorbency and superhydrophobicity ensures its application for the cleanup of oil from water. It is worthy to note that no measurable weight loss of the samples was detected after being soaked in the organics for a long time or repeated absorption tests. This is attributed to the tight binding of the coating to the sponge and the inherent stability of the coating toward solvents.

CONCLUSIONS

In summary, a facile strategy for preparing magnetic, durable, and superhydrophobic PU@Fe₃O₄@SiO₂@FP sponges was developed by CVD of TEOS in the presence of the Fe₃O₄ NPs and then dip-coating in a FP aqueous solution. The CVD of

TEOS forms a thin layer of SiO₂, which immobilizes the Fe₃O₄ NPs on the skeleton of the PU sponge. The in turn binding of Fe₃O₄ NPs, SiO₂ layer, and FP on the surface of the PU sponges not only endows the sponges with magnetic responsivity and superhydrophobicity/superoleophilicity but also improves the elongation at break. The sponge features the merits of magnetic actuation, high mechanical and chemical stabilities, as well as excellent superhydrophobicity/superoleophilicity. In addition, the sponge could be magnetically driven to the polluted water zone using a magnet, quickly absorb floating oils on water surface and heavy oils under water, and act as a membrane for oil/water separation. Moreover, the sponge shows very high selectivity in oil/water separation. With the help of a vacuum pump, the sponge can be used for the continuous separation of large amounts of oil pollutants from the water surface, which makes it a very promising material for practical oil absorption and oil/water separation in a feasible and energy-efficient way. The sponge could maintain its superhydrophobicity and oil absorbency after intensive stretching and compression, long time immersion in various oils, and repeated oil absorption. The superior mechanical stability and stability in oil of the superhydrophobic PU sponges to most of the reported superhydrophobic materials pave the way for their applications in selective oil absorption and oil/water separation.

ASSOCIATED CONTENT

Supporting Information

Typical image of a water drop on the superhydrophobic sponge, the principle setup for WSA measurement, Fe₃O₄ NPs falling off the PU@Fe₃O₄ sponge, magnetic curve of Fe₃O₄ NPs, recycle of the sponge using a magnet, images of the sponges held by magnets after used for ten cycles, physical parameters of the organics used in this study and oil absorbency of the for these organics, comparison of various oil absorbents, and videos. This material is available free of charge via the Internet at <http://pubs.acs.org>.

AUTHOR INFORMATION

Corresponding Authors

* E-mail: jjpzhang@licp.cas.cn.

* E-mail: aqwang@licp.cas.cn.

Author Contributions

The manuscript was written through contributions of all authors. All authors have given approval to the final version of the manuscript.

Notes

The authors declare no competing financial interest.

ACKNOWLEDGMENTS

We are grateful for financial support of the “Hundred Talents Program” of the Chinese Academy of Sciences, the open funding (CASXY2013-02) the Xuyi Center of Attapulgite Applied Technology Research Development & Industrialization of the Chinese Academy of Sciences, and the Key Technology R&D Program of Jiangsu (BE2014102).

REFERENCES

- (1) Zhang, J. P.; Seeger, S. Polyester Materials with Superwetting Silicone Nanofilaments for Oil/Water Separation and Selective Oil Absorption. *Adv. Funct. Mater.* **2011**, *21*, 4699–4704.
- (2) Liu, M. J.; Zheng, Y. M.; Zhai, J.; Jiang, L. Bioinspired Super-Antiwetting Interfaces with Special Liquid-Solid Adhesion. *Acc. Chem. Res.* **2010**, *43*, 368–377.
- (3) Levkin, P. A.; Svec, F.; Fréchet, J. M. J. Porous Polymer Coatings: A Versatile Approach to Superhydrophobic Surfaces. *Adv. Funct. Mater.* **2009**, *19*, 1993–1998.
- (4) Xue, Z.; Wang, S.; Lin, L.; Chen, L.; Liu, M.; Feng, L.; Jiang, L. A Novel Superhydrophilic and Underwater Superoleophobic Hydrogel-Coated Mesh for Oil/Water Separation. *Adv. Mater.* **2011**, *23*, 4270–4273.
- (5) Zhang, W. B.; Shi, Z.; Zhang, F.; Liu, X.; Jin, J.; Jiang, L. Superhydrophobic and Superoleophilic PVDF Membranes for Effective Separation of Water-in-Oil Emulsions with High Flux. *Adv. Mater.* **2013**, *25*, 2071–2076.
- (6) Wang, C.; Yao, T.; Wu, J.; Ma, C.; Fan, Z.; Wang, Z.; Cheng, Y.; Lin, Q.; Yang, B. Facile Approach in Fabricating Superhydrophobic and Superoleophilic Surface for Water and Oil Mixture Separation. *ACS Appl. Mater. Interfaces* **2009**, *1*, 2613–2617.
- (7) Wu, J.; Wang, N.; Wang, L.; Dong, H.; Zhao, Y.; Jiang, L. Electrospun Porous Structure Fibrous Film with High Oil Adsorption Capacity. *ACS Appl. Mater. Interfaces* **2012**, *4*, 3207–3212.
- (8) Zhang, X. Y.; Li, Z.; Liu, K. S.; Jiang, L. Bioinspired Multifunctional Foam with Self-Cleaning and Oil/Water Separation. *Adv. Funct. Mater.* **2013**, *23*, 2881–2886.
- (9) Kota, A. K.; Kwon, G.; Choi, W.; Mabry, J. M.; Tuteja, A. Hygro-Responsive Membranes for Effective Oil-Water Separation. *Nat. Commun.* **2012**, *3*, 1025.
- (10) Yuan, J.; Liu, X.; Akbulut, O.; Hu, J.; Suib, S. L.; Kong, J.; Stellacci, F. Superwetting Nanowire Membranes for Selective Absorption. *Nat. Nanotechnol.* **2008**, *3*, 332–336.
- (11) Lahann, J. Environmental Nanotechnology: Nanomaterials Clean Up. *Nat. Nanotechnol.* **2008**, *3*, 320–321.
- (12) Inagaki, M.; Kawahara, A.; Nishi, Y.; Iwashita, N. Heavy Oil Sorption and Recovery by Using Carbon Fiber Felts. *Carbon* **2002**, *40*, 1487–1492.
- (13) Liang, H. W.; Guan, Q. F.; Chen, L. F.; Zhu, Z.; Zhang, W. J.; Yu, S. H. Macroscopic-Scale Template Synthesis of Robust Carbonaceous Nanofiber Hydrogels and Aerogels and Their Applications. *Angew. Chem., Int. Ed.* **2012**, *51*, 5101–5105.
- (14) Bi, H. C.; Xie, X.; Yin, K. B.; Zhou, Y. L.; Wan, S.; He, L. B.; Xu, F.; Banhart, F.; Sun, L. T.; Ruoff, R. S. Spongy Graphene as a Highly Efficient and Recyclable Sorbent for Oils and Organic Solvents. *Adv. Funct. Mater.* **2012**, *22*, 4421–4425.
- (15) Gui, X. C.; Wei, J. Q.; Wang, K. L.; Cao, A. Y.; Zhu, H. W.; Jia, Y.; Shu, Q. K.; Wu, D. H. Carbon Nanotube Sponges. *Adv. Mater.* **2010**, *22*, 617–621.
- (16) Shi, M. K.; Oh, J.; Lima, M.; Kozlov, M. E.; Kim, S. J.; Baughman, R. H. Elastomeric Conductive Composites Based on Carbon Nanotube Forests. *Adv. Mater.* **2010**, *22*, 2663–2667.
- (17) Xu, Y. X.; Sheng, K. X.; Li, C.; Shi, G. Q. Self-Assembled Graphene Hydrogel via a One-Step Hydrothermal Process. *ACS Nano* **2010**, *4*, 4324–4330.
- (18) Bi, H. C.; Yin, K. B.; Xie, X.; Zhou, Y. L.; Wan, N.; Xu, F.; Banhart, F.; Sun, L. T.; Ruoff, R. S. Low Temperature Casting of Graphene with High Compressive Strength. *Adv. Mater.* **2012**, *24*, 5124–5129.
- (19) Wang, S. H.; Li, M.; Lu, Q. H. Filter Paper with Selective Absorption and Separation of Liquids That Differ in Surface Tension. *ACS Appl. Mater. Interface* **2010**, *2*, 677–683.
- (20) Zang, D. M.; Wu, C. X.; Zhu, R. W.; Zhang, W.; Yu, X. Q.; Zhang, Y. F. Porous Copper Surfaces with Improved Superhydrophobicity under Oil and Their Application in Oil Separation and Capture from Water. *Chem. Commun.* **2013**, *49*, 8410–8412.
- (21) Cheng, Z. J.; Lai, H.; Du, Y.; Fu, K. W.; Hou, R.; Zhang, N. Q.; Sun, K. N. Underwater Superoleophilic to Superoleophobic Wetting Control on the Nanostructured Copper Substrates. *ACS Appl. Mater. Interfaces* **2013**, *5*, 11363–11370.
- (22) Tian, D.; Zhang, X.; Tian, Y.; Wu, Y.; Wang, X.; Zhai, J.; Jiang, L. Photo-Induced Water-Oil Separation Based on Switchable Superhydrophobicity-Superhydrophilicity and Underwater Superoleophobicity of the Aligned ZnO Nanorod Array-Coated Mesh Films. *J. Mater. Chem.* **2012**, *22*, 19652–19657.
- (23) Xue, Z. X.; Wang, S. T.; Lin, L.; Chen, L.; Liu, M. J.; Feng, L.; Jiang, L. A Novel Superhydrophilic and Underwater Superoleophobic Hydrogel-Coated Mesh for Oil/Water Separation. *Adv. Mater.* **2011**, *23*, 4270–4273.
- (24) Lee, C.; Baik, S. Vertically-Aligned Carbon Nano-Tube Membrane Filters with Superhydrophobicity and Superoleophilicity. *Carbon* **2010**, *48*, 2192–2197.
- (25) Calcagnile, P.; Fragouli, D.; Bayer, I. S.; Anyfantis, G. C.; Martiradonna, L.; Cozzoli, P. D.; Cingolani, R.; Athanassiou, A. Magnetically Driven Floating Foams for The Removal of Oil Contaminants from Water. *ACS Nano* **2012**, *6*, 5413–5419.
- (26) Zhu, Q.; Pan, Q. M.; Liu, F. T. Facile Removal and Collection of Oils from Water Surfaces through Superhydrophobic and Superoleophilic Sponges. *J. Phys. Chem. C* **2011**, *115*, 17464–17470.
- (27) Wang, B.; Li, J.; Wang, G. Y.; Liang, W. X.; Zhang, Y. B.; Shi, L.; Guo, Z. G.; Liu, W. M. Methodology for Robust Superhydrophobic Fabrics and Sponges from In Situ Growth of Transition Metal/Metal Oxide Nanocrystals with Thiol Modification and Their Applications in Oil/Water Separation. *ACS Appl. Mater. Interfaces* **2013**, *5*, 1827–1839.
- (28) Li, J.; Shi, L.; Chen, Y.; Zhang, Y. B.; Guo, Z. G.; Su, B. L.; Liu, W. M. Stable Superhydrophobic Coatings from Thiol-Ligand Nanocrystals and Their Application in Oil/Water Separation. *J. Mater. Chem.* **2012**, *22*, 9774–9781.
- (29) Zhu, Q.; Chu, Y.; Wang, Z. K.; Chen, N.; Lin, L.; Liu, F. T.; Pan, Q. M. Robust Superhydrophobic Polyurethane Sponge As a Highly Reusable Oil-Absorption Material. *J. Mater. Chem. A* **2013**, *1*, 5386–5393.
- (30) Liu, Y.; Ma, J. K.; Wu, T.; Wang, X. R.; Huang, G. B.; Liu, Y.; Qiu, H. X.; Li, Y.; Wang, W.; Gao, J. P. Cost-Effective Reduced Graphene Oxide-Coated Polyurethane Sponge As a Highly Efficient and Reusable Oil-Absorbent. *ACS Appl. Mater. Interfaces* **2013**, *5*, 10018–10026.
- (31) Liu, F. T.; Sun, F. H.; Pan, Q. M. Highly Compressible and Stretchable Superhydrophobic Coating Inspired by Bioadhesion of Marine Mussels. *J. Mater. Chem. A* **2014**, *2*, 11365–11371.
- (32) Peng, L.; Yuan, S.; Yan, G.; Yu, P.; Luo, Y. B. Hydrophobic Sponge for Spilled Oil Absorption. *J. Appl. Polym. Sci.* **2014**, *131*, 40886.
- (33) Sun, Z. H.; Wang, L. F.; Liu, P. P.; Wang, S. C.; Sun, B.; Jiang, D. Z.; Xiao, F. S. Magnetically Motive Porous Sphere Composite and Its Excellent Properties for The Removal of Pollutants in Water by Adsorption and Desorption Cycles. *Adv. Mater.* **2006**, *18*, 1968–1971.

- (34) Zhu, Q.; Tao, F.; Pan, Q. M. Fast and Selective Removal of Oils from Water Surface via Highly Hydrophobic Core Shell $\text{Fe}_2\text{O}_3/\text{C}$ Nanoparticles under Magnetic Field. *ACS Appl. Mater. Interfaces* **2010**, *2*, 3141–3146.
- (35) Xu, L. P.; Wu, X.; Meng, J.; Peng, J.; Wen, Y.; Zhang, X.; Wang, S. Papilla-Like Magnetic Particles with Hierarchical Structure for Oil Removal from Water. *Chem. Commun.* **2013**, *49*, 8752–8754.
- (36) Pavía-Sanders, A.; Zhang, S.; Flores, J. A.; Sanders, J. E.; Raymond, J. E.; Wooley, K. L. Robust Magnetic/Polymer Hybrid Nanoparticles Designed for Crude Oil Entrapment and Recovery in Aqueous Environments. *ACS Nano* **2013**, *7*, 7552–7561.
- (37) Calcagnile, P.; Fragouli, D.; Bayer, I. S.; Anyfantis, G. C.; Martiradonna, L.; Cozzoli, P. D.; Cingolani, R.; Athanassiou, A. Magnetically Driven Floating Foams for The Removal of Oil Contaminants from Water. *ACS Nano* **2012**, *6*, 5413–5419.
- (38) Chen, N.; Pan, Q. M. Versatile Fabrication of Ultralight Magnetic Foams and Application for Oil-Water Separation. *ACS Nano* **2013**, *7*, 6875–6883.
- (39) Li, L.; Li, B.; Wu, L.; Zhao, X.; Zhang, J. Magnetic, Superhydrophobic and Durable Silicone Sponges and Their Applications in Removal of Organic Pollutants from Water. *Chem. Commun.* **2014**, *50*, 7831–7833.
- (40) Zhang, J. P.; Li, B. C.; Wu, L.; Wang, A. Q. Facile Preparation of Durable and Robust Superhydrophobic Textiles by Dip Coating in Nanocomposite Solution of Organosilanes. *Chem. Commun.* **2013**, *49*, 11509–11511.
- (41) Wu, L.; Zhang, J. P.; Li, B. C.; Wang, A. Q. Mimic Nature, Beyond Nature: Facile Synthesis of Durable Superhydrophobic Textiles Using Organosilanes. *J. Mater. Chem. B* **2013**, *1*, 4756–4763.
- (42) Li, W.; Deng, Y. H.; Wu, Z. X.; Qian, X. F.; Yang, J. P.; Wang, Y.; Gu, D.; Zhang, F.; Tu, B.; Zhao, D. Y. Hydrothermal Etching Assisted Crystallization: A Facile Route to Functional Yolk-Shell Titanate Microspheres with Ultrathin Nanosheets-Assembled Double Shells. *J. Am. Chem. Soc.* **2011**, *133*, 15830–15833.
- (43) Deng, H.; Li, X. L.; Peng, Q.; Wang, X.; Chen, J. P.; Li, Y. D. Monodisperse Magnetic Single-Crystal Ferrite Microspheres. *Angew. Chem., Int. Ed.* **2005**, *44*, 2782–2785.
- (44) Zimmermann, J.; Reifler, F. A.; Fortunato, G.; Gerhardt, L. C.; Seeger, S. A Simple, One-Step Approach to Durable and Robust Superhydrophobic Textiles. *Adv. Funct. Mater.* **2008**, *18*, 3662–3669.
- (45) Zimmermann, J.; Seeger, S.; Reifler, F. A. Water Shedding Angle: A New Technique to Evaluate the Water-Repellent Properties of Superhydrophobic Surfaces. *Text. Res. J.* **2009**, *79*, 1565–1570.
- (46) Deng, X.; Mammen, L.; Butt, H. J.; Vollmer, D. Candle Soot as a Template for a Transparent Robust Superamphiphobic Coating. *Science* **2012**, *335*, 67–70.
- (47) Ding, H. L.; Zhang, Y. X.; Wang, S.; Xu, J. M.; Xu, S. C.; Li, G. H. $\text{Fe}_3\text{O}_4/\text{SiO}_2$ Core/Shell Nanoparticles: The Silica Coating Regulations with a Single Core for Different Core Sizes and Shell Thicknesses. *Chem. Mater.* **2012**, *24*, 4572–4580.
- (48) Chen, H. M.; Deng, C. H.; Zhang, X. M. Synthesis of $\text{Fe}_3\text{O}_4/\text{SiO}_2/\text{PMMA}$ Core-Shell-Shell Magnetic Microspheres for Highly Efficient Enrichment of Peptides and Proteins for MALDI-ToF MS Analysis. *Angew. Chem., Int. Ed.* **2010**, *49*, 607–611.
- (49) Chen, F. H.; Gao, Q.; Ni, J. Z. The Grafting and Release Behavior of Doxorubicin from $\text{Fe}_3\text{O}_4/\text{SiO}_2$ Core-Shell Structure Nanoparticles via an Acid Cleaving Amide Bond: The Potential for Magnetic Targeting Drug Delivery. *Nanotechnology* **2008**, *19*, 165103–165111.
- (50) Hu, H. B.; Wang, Z. H.; Pan, L.; Zhao, S. P.; Zhu, S. Y. Ag-Coated $\text{Fe}_3\text{O}_4/\text{SiO}_2$ Three-Ply Composite Microspheres: Synthesis, Characterization, and Application in Detecting Melamine with Their Surface-Enhanced Raman Scattering. *J. Phys. Chem. C* **2010**, *114*, 7738–7742.
- (51) Lien, Y. H.; Wu, T. M. Preparation and Characterization of Thermosensitive Polymers Grafted onto Silica-Coated Iron Oxide Nanoparticles. *J. Colloid Interface Sci.* **2008**, *326*, 517–521.
- (52) Shimizu, K.; Phanopoulos, C.; Loenders, R.; Abel, M. L.; Watts, J. F. The Characterization of the Interfacial Interaction between Polymericmethylene Diphenyl Diisocyanate and Aluminum: A ToF-SIMS and XPS Study. *Surf. Interface Anal.* **2010**, *42*, 1432–1444.
- (53) Montes, M.; Getton, F. P.; Vong, M. S. W.; Sermon, P. A. Titania on Silica. A Comparison of Sol-Gel Routes and Traditional Methods. *J. Sol-Gel Sci. Technol.* **1997**, *8*, 131–137.
- (54) Barr, T. L. An ESCA Study of The Termination of The Passivation of Elemental Metals. *J. Phys. Chem.* **1978**, *82*, 1801–1810.
- (55) Mackie, N. M.; Castner, D. G.; Fisher, E. R. Characterization of Pulsed-Plasma-Polymerized Aromatic Films. *Langmuir* **1998**, *14*, 1227–1235.
- (56) Fang, J.; Wang, H.; Xue, Y.; Wang, X.; Lin, T. Magnet-Induced Temporary Superhydrophobic Coatings from One-Pot Synthesized Hydrophobic Magnetic Nanoparticles. *ACS Appl. Mater. Interfaces* **2010**, *2*, 1449–55.
- (57) Li, A.; Sun, H. X.; Tan, D. Z.; Fan, W. J.; Wen, S. H.; Qing, X. J.; Li, G. X.; Lia, S. Y.; Deng, W. Q. Superhydrophobic Conjugated Microporous Polymers for Separation and Adsorption. *Energy Environ. Sci.* **2011**, *4*, 2062–2065.
- (58) Jiang, G.; Hu, R.; Xi, X.; Wang, X.; Wang, R. Facile Preparation of Superhydrophobic and Superoleophilic Sponge for Fast Removal of Oils from Water Surface. *J. Mater. Res.* **2013**, *28*, 651–656.